Physics and Imaging in Radiation Oncology 19 (2021) 1–5

Contents lists available at ScienceDirect

Physics and Imaging in Radiation Oncology

journal homepage: www.sciencedirect.com/journal/physics-and-imaging-in-radiation-oncology

Out-of-field dose in stereotactic radiotherapy for paediatric patients

Lachlan Garrett [a,b], Nicholas Hardcastle [b,c], Adam Yeo [b], Peta Lonski [b], Rick Franich [a], Tomas Kron [a,b,c,*]

[a] RMIT University, School of Science, Melbourne, Australia
[b] Peter MacCallum Cancer Centre, Department of Physical Sciences, Melbourne, Australia
[c] University of Wollongong, Centre for Medical Radiation Physics, Wollongong, Australia

ARTICLE INFO

Keywords:
SABR
Paediatric
Out-of-field dose
Peripheral dose
High dose rate

ABSTRACT

Background and purpose: Stereotactic radiotherapy combines image guidance and high precision delivery with small fields to deliver high doses per fraction in short treatment courses. In preparation for extension of these treatment techniques to paediatric patients we characterised and compared doses out-of-field in a paediatric anthropomorphic phantom for small flattened and flattening filter free (FFF) photon beams.

Method and materials: Dose measurements were taken in several organs and structures outside the primary field in an anthropomorphic phantom of a 5 year old child (CIRS) using thermoluminescence dosimetry (LiF:Mg,Cu,P). Out-of-field doses from a medical linear accelerator were assessed for 6 MV flattened and FFF beams of field sizes between 2×2 and 10×10 cm^2.

Results: FFF beams resulted in reduced out-of-field doses for all field sizes when compared to flattened beams. Doses for FFF and flattened beams converged for all field sizes at larger distances (>40 cm) from the central axis as leakage becomes the primary source of out-of-field dose. Rotating the collimator to place the MLC bank in the longitudinal axis of the patient was shown to reduce the peripheral doses measured by up to 50% in Varian linear accelerators.

Conclusion: Minimising out-of-field doses by using FFF beams and aligning the couch and collimator to provide tertiary shielding demonstrated advantages of small field, FFF treatments in a paediatric setting.

1. Introduction

Globally, cancer is one of the leading causes of death in children aged 0–19 years old, with approximately 300,000 new cases diagnosed each year [1]. The use of radiotherapy in children has fluctuated over the years and at present up to one third of children receive radiation therapy as a part of their cancer treatment [2]. While historically stereotactic radiotherapy procedures were mostly reserved for arterio-venous malformations (AVM) [3] there is an increasing interest to also extend the use of stereotactic ablative body radiotherapy (SABR) to childhood cancers [4,5]. Out-of-field radiation dose is of particular concern in the context of children who are more prone to radiation induced secondary cancers [6], a fact that has been a major driver for the interest in proton radiotherapy [7]. While areas surrounding the primary beam receive the majority of out-of-field dose, there are structures that receive dose from internal scatter and leakage beyond regions where the treatment planning system (TPS) can calculate dose accurately [8,9]. In the context of high precision radiotherapy which relies on image guidance such as SABR this effect is compounded by the associated imaging dose [10].

Out-of-field doses from linear accelerators in radiotherapy have been studied by many authors with several reviews providing summaries [11–13]. However, there is little published specifically on paediatric treatment scenarios with most of the papers specific to clinical treatment scenarios such as for brain lesions [14,15] including an EURADOS study on out-of-field doses from IMRT and Gammaknife in AVMs [16]. We are aiming to add to this by specifically addressing out-of-field dose to paediatric patients from small fields such as that which may be used in SABR treatments. Of particular interest in this context is the use of flattening filter free (FFF) beams [17,18]. Therefore, the aim of this study was to measure out-of-field dose in an anthropomorphic paediatric phantom for different target locations and small field sizes, comparing flattened and FFF beams.

* Corresponding author at: Department of Physical Sciences, Peter MacCallum Cancer Centre, 305 Grattan Street, Melbourne, VIC 3000, Australia.
E-mail address: Tomas.Kron@petermac.org (T. Kron).

https://doi.org/10.1016/j.phro.2021.05.006
Received 22 December 2020; Received in revised form 18 May 2021; Accepted 22 May 2021
Available online 4 June 2021

Table 1
Thermoluminescence dosimeter locations (organs) and distances from the central axis for all four radiotherapy field sites.

	Distance from the field centre (cm)			
Measurement location	Brain	Neck	Thorax	Abdomen
Brain	–	15.2	25.2	39.9
Thyroid	15.2	–	10.2	24.7
Heart	25.0	9.9	2.7	14.8
Lung	25.9	11.8	9.1	16.1
Abdomen	39.9	24.7	15.1	–
Gonads	52.5	37.3	27.6	12.6

2. Method and materials

2.1. Phantom and dosimetry

Thermoluminescence dosimetry measurements were conducted using a phantom of a five-year-old paediatric patient (CIRS, Norfolk, USA) made from tissue equivalent materials including bone, soft tissue, and lung. The phantom featured 5 mm diameter holes spaced in a 3 × 3 cm^2 grid in each phantom slice for dosimetry using Thermoluminescence Dosimeters (TLDs). Individually calibrated LiF:Mg,Cu,P TLD-100H chips (3.1 × 3.1 × 0.9 mm^3, Harshaw, Ohio, USA) were used due to their high sensitivity and wide dosimetric range [19]. A Harshaw 5500 automatic TLD reader was used for readout using nitrogen gas heating, a pre-read anneal of 10 s at 150 °C and a readout temperature of 250 °C. All TLDs were annealed after each use for 30 min at 240 °C.

For the measurements, TLDs were placed in the anatomical locations of the brain, thyroid, heart, lung, abdomen, and gonads as indicated in Table 1. The TLDs were placed in the same coronal and sagittal planes with the exception of the heart and (right) lung which were placed off centre to correspond to organ location.

The reproducibility of the each TLD measurement in reference conditions was better than 2% at 95% confidence interval (CI). Using five TLDs from the same batch as standards irradiated to a known dose (typically 100 mGy) at depth of maximum dose in a 10 × 10 cm^2 field of 6 MV X-rays and two TLDs per measurement point resulted in an overall uncertainty of ± 5% at 95% CI for a given dose readout [20,21].

2.2. Irradiation

Out-of-field measurements were taken in the paediatric phantom at six locations as listed in Table 1. The phantom was set up in the head-first supine position and four different field sites were irradiated: brain, neck, thorax, and abdomen. The field sites and measurement locations are listed in Table 1 and illustrated in Fig. 1. All irradiations were performed with a Varian TrueBeam STx (Varian, Palo Alto, USA) with an HD120 MLC. For each field location, beams were delivered with jaw-

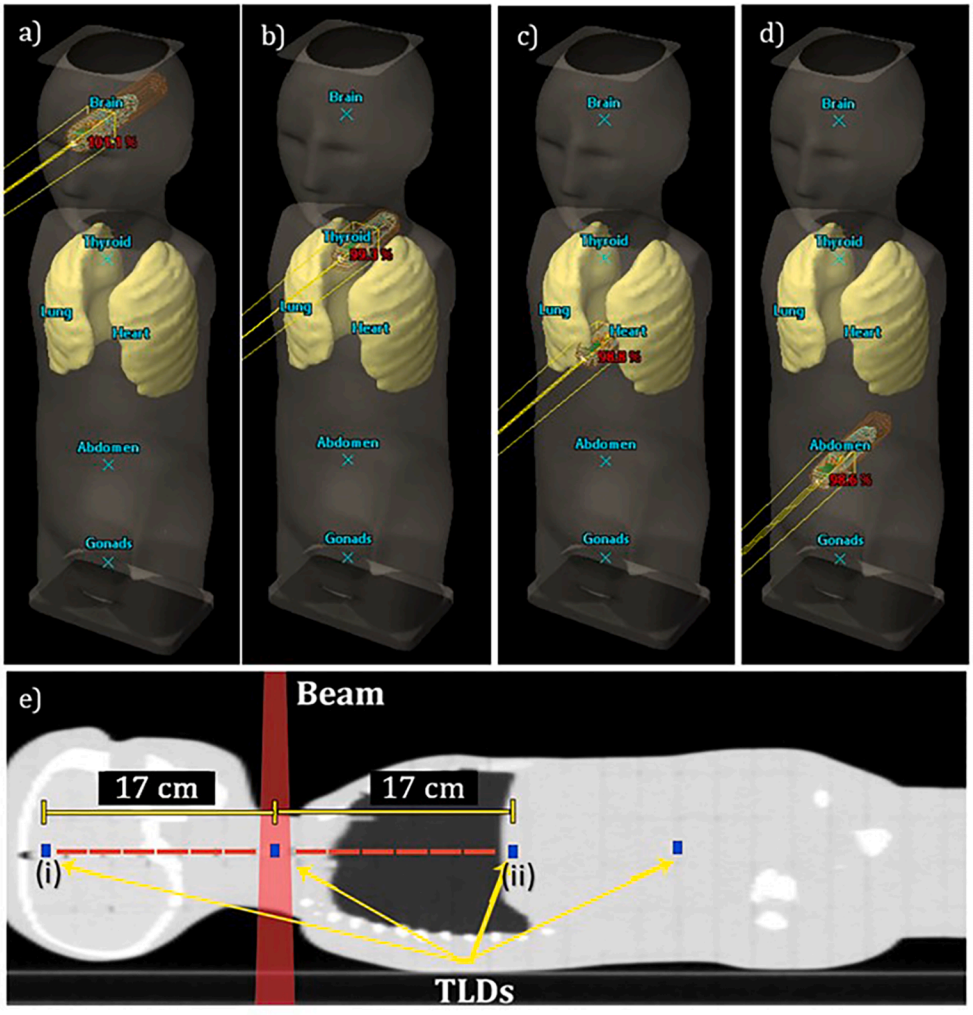

Fig. 1. Schematic representing the four different field locations used in the present study: (a) brain, (b) neck, (c) thorax, and (d) abdomen. Shown are the 2 × 2 cm^2 fields. Additional field sizes of 5 × 5 cm^2 and 10 × 10 cm^2 were also used. TLDs were placed at each labelled anatomical location. (e) shows two measurement points at equal distances from the beam (i) and (ii) but with different radiological path lengths due to inhomogeneities.

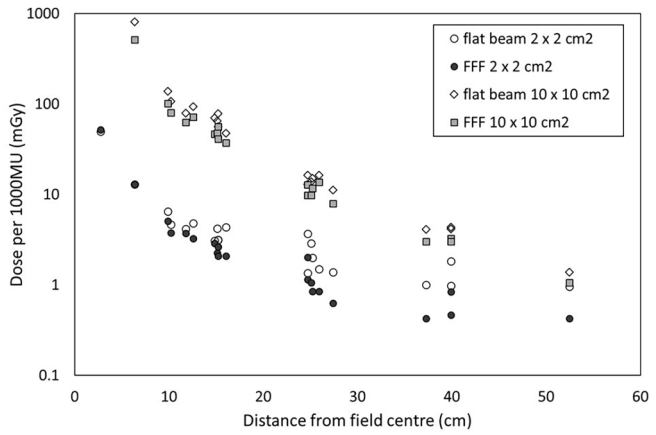

Fig. 2. Out-of-field doses for two field sizes using a 6MV X-ray beam in flattened and flattening filter free (FFF) mode as a function of the distance from the field centre.

defined 10 × 10 cm^2, 5 × 5 cm^2 (MLC retracted), and MLC-defined 2 × 2 cm^2 field sizes. For the 2 × 2 cm^2 field the jaws were set to 3 × 3 cm^2 which reflects typical commissioning conditions for the Varian Eclipse treatment planning system used in our institution. The largest field size was used as reference. The collimator rotation was 90° except where otherwise specified. To quantify the additional shielding provided by the MLC bank, additional measurements were performed for 5 × 5 cm^2 abdominal fields with the collimator oriented at both 0° and 90°. All exposures were delivered with 100 MU, operated at 6 MV and 6 MV Flattening Filter Free (FFF). TPR^{20}_{10} for the two beams was 0.6678 and 0.6315, respectively.

3. Results

Measured out-of-field dose reduced with distance from the field centre as shown in Fig. 2 for two of the three field sizes for a 6 MV X-ray flattened beam and a 6 MV FFF beam. As can be seen in Fig. 1 there were circumstances where field position and detector locations were exchanged (for example, dose from abdominal field to thyroid and dose from thyroid field to abdomen). This should lead to similar doses in both treatment scenarios as the radiological distance between field centre and TLD position is similar even if scatter conditions vary. In the six exchangeable locations probed over 3 field sizes and for both flattened and FFF beams the average ratio of dose received in the two scenarios where field centre and TLD position were exchanged was 1.12 ± 0.39 (1 SD).

The difference between out-of-field dose for the flattened beam and the FFF beam of the same size was found to increase with distance from the field. The variation in out-of-field dose for similar distances from the field centre in the same beam as shown in Fig. 2 can be attributed to the use of an anthropomorphic phantom. This was shown by comparing dose in locations where lung was located between field and measurement location, to dose where the direct path was through tissue only (as illustrated in Fig. 1). Fig. 3 shows this for a 2 × 2 cm^2 field. A tendency was found that dose behind lung was larger than behind tissue.

In the smallest field the dose was found to decrease faster with distance from the field in an FFF beam compared to a flattened beam. This is shown in Fig. 4, which shows the ratio of out-of-field doses from FFF beams to flattened beams for all 3 field sizes as a function of distance from the central axis. For the 5 × 5 cm^2 and 10 × 10 cm^2 fields, the ratio of doses between FFF and flattened fields was found to be largely independent of distance. The ratio was found to be below 1 as the overall number of photons delivered is smaller for FFF beams when both fields are normalised at central axis.

In the smallest field size, head leakage outside of the field dominated over phantom scatter and as such the change with distance reflected the shape of the primary dose profile. The beam profile of the 6MV photon beam for FFF reached approximately 50% 20 cm away from central axis, which was similar to the reduction of the dose ratio in Fig. 4.

In the studied linear accelerator the collimator angle was also found to influence out-of-field doses. Fig. 5 shows the out-of-field dose with the collimator angles of 0° and 90° for measurements using a flattened beam. The reduction of leakage dose at a distance of 20 cm was of the order of 50% when the collimator was set to 90°.

4. Discussion

Out-of-field dose is composed of leakage, collimator and patient scatter [13]. The variation in measurements at the same distance from the field edge was related to the location of the field relative to the

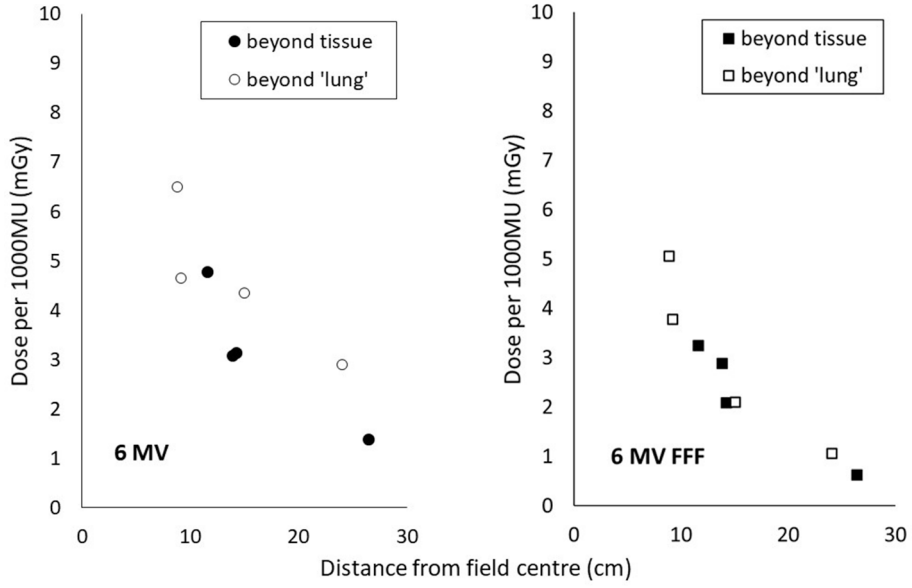

Fig. 3. Comparison of out-of-field dose behind lung and tissue for a 2 × 2 cm^2 field of 6MV X-rays with and without flattening filter. The out-of-field doses in the FFF beams were lower than for the flattened beams shown in the left panel.

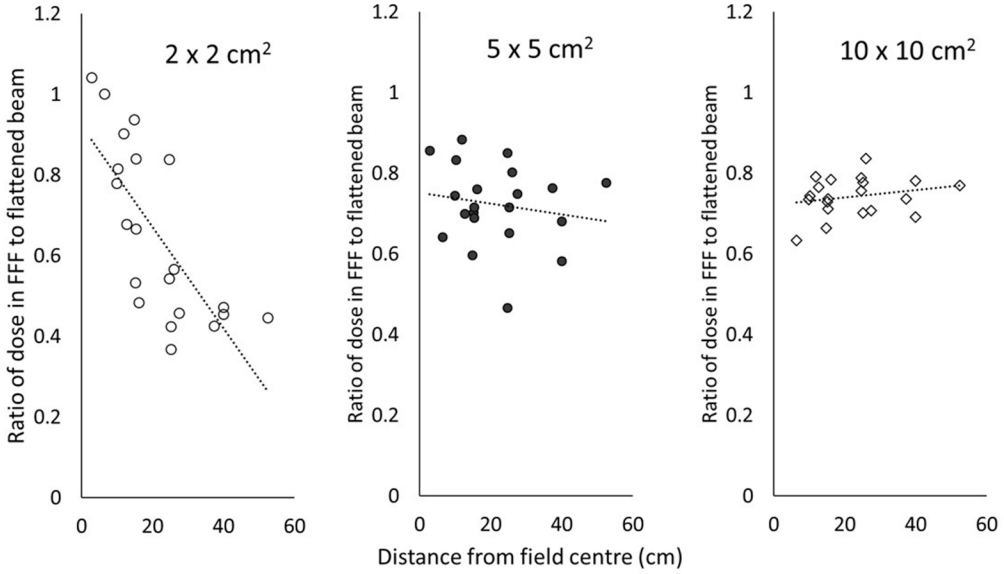

Fig. 4. Variation of the ratio between out-of-field dose in FFF beams compared to flattened beams as a function of field size and distance from the field centre. While the data show a lower out-of-field dose for the FFF beam (ratio < 1), there was a significant reduction of dose ratio with distance from the field centre only in case of the smallest field size.

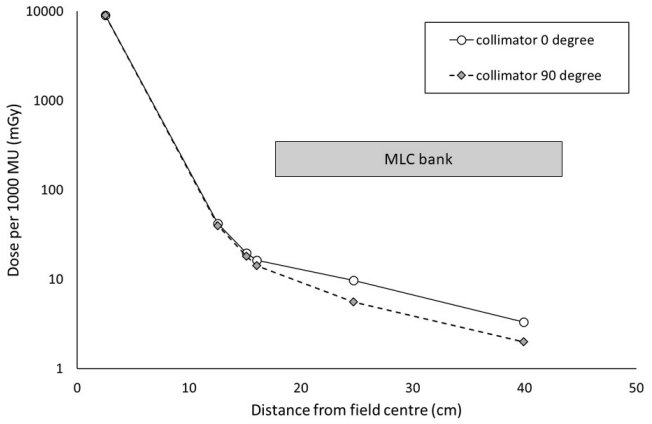

Fig. 5. Out-of-field doses from abdominal 5 × 5 cm^2 fields at various distances from the field edge using a flattened beam and different collimator angles. The location of the MLC bank in case of 90° collimator rotation is indicated.

measurement point in the phantom. While several studies have investigated this in homogenous phantoms [12,22,23] we investigated out-of-field doses in a more realistic scenario using an anthropomorphic phantom. There was a lack of full and symmetric scatter conditions, and low-density structures such as lung affected the radiological path length of the scattered radiation. Fig. 1e shows an example of scattered radiation paths that traverse tissue and/or lung. As out-of-field dose is more concerning for late effects in children [10,24] an anthropomorphic phantom was chosen that mimics a 5 year old in size and body composition. A limitation of our study was that only static fields symmetric around central axis (CAX) were explored. It can be expected that the complexity increases further if modulated arc treatments are used.

For both flattened and FFF beams larger field sizes resulted in greater out-of-field doses at small distances from CAX where phantom scatter dominates as illustrated in Fig. 2. However, when the distance from the CAX was increased the dependence on field size is reduced as leakage becomes more important [21,25]. The data shown in Fig. 4 for the smallest field size demonstrates this as phantom scatter was small and the difference between flattened and FFF beam reflected the beam profiles behind MLC and collimator. Close to the field edge, patient and collimator scatter were found to be dependent on the field size which causes the large differences between the doses for different field sizes [26,27].

Two components contributed to the reduction in out-of-field dose in FFF beams compared to flattened beams: (i) the removal of a major scattering component source, the flattening filter [28], and (ii) the fact that all beams were normalised at central axis which will lead to less primary photons in the periphery for FFF beams resulting in lower transmission through the collimation system.

Fig. 5 shows the ratio of the dose with the collimator at 0° to that at 90° as a function of distance from the field centre. One technique for dose reduction in Varian linear accelerators is to rotate the collimator to align the MLC bank to the longitudinal axis of patient which reduces the dose in a 6MV beam by half for distances greater than 15 cm from the field edge [15].

The work presented in the present study confirmed that the use of FFF beams for SABR treatments can deliver lower out-of-field doses overall compared to their flattening filter beam counterparts [26,28]. This will not only reduce the probability of developing a second cancer but also other late effects such as cardiac toxicity as a result of the radiation exposure.[29,30] All this is particularly important for paediatric patients and was shown to hold in the complex dose distributions observed in anthropomorphic phantoms.

Declaration of Competing Interest

The authors declare the following financial interests/personal relationships which may be considered as potential competing interests: Tomas Kron and Nicholas Hardcastle are coinvestigators in an unrelated research collaboration with Varian Medical Systems

Acknowledgements

This work was supported by funding from the CASS foundation for our SABR in children program and is greatly appreciated. We thank Chris Fox and Elena Ungureanu for their help throughout this project and acknowledge the support of the Gross Foundation for the dosimetry aspects of the work.

References

[1] Steliarova-Foucher E, Colombet M, Ries LAG, Moreno F, Dolya A, Bray F, et al. International incidence of childhood cancer, 2001–10: a population-based registry study. Lancet Oncol 2017;18(6):719–31.

[2] Bishr MK, Zaghloul MS, Elmaraghi C, Galal A, Abdelaziz MS, Elghazawy HI, et al. The radiotherapy utilization rate in pediatric tumors: An analysis of 13,305 patients. Radiother Oncol 2021;154:220–6.

[3] Borcek AO, Celtikci E, Aksogan Y, Rousseau MJ. Clinical Outcomes of Stereotactic Radiosurgery for Cerebral Arteriovenous Malformations in Pediatric Patients: Systematic Review and Meta-Analysis. Neurosurgery. 2019;85:E629-E40.

[4] Elledge CR, Krasin MJ, Ladra MM, Alcorn SR, Han P, Gibbs IC, et al. A multi-institutional phase 2 trial of stereotactic body radiotherapy in the treatment of bone metastases in pediatric and young adult patients with sarcoma. Cancer 2021; 127(5):739–47.

[5] Tinkle CL, Singh C, Lloyd S, Guo Y, Li Y, Pappo AS, et al. Stereotactic body radiotherapy for metastatic and recurrent solid tumors in children and young adults. Int J Radiat Oncol Biol Phys 2021;109:1396–405.

[6] Ng J, Shuryak I. Minimizing second cancer risk following radiotherapy: current perspectives. Cancer Manag Res 2015;7:1–11.

[7] Zhang R, Howell RM, Giebeler A, Taddei PJ, Mahajan A, Newhauser WD. Comparison of risk of radiogenic second cancer following photon and proton craniospinal irradiation for a pediatric medulloblastoma patient. Phys Med Biol 2013;58(4):807–23.

[8] Huang JY, Followill DS, Wang XA, Kry SF. Accuracy and sources of error of out-of field dose calculations by a commercial treatment planning system for intensity-modulated radiation therapy treatments. J Appl Clin Med Phys 2013;14(2):186–97.

[9] Lonski P, Kron T, Taylor M, Phipps A, Franich R, Chua B. Assessment of leakage dose in vivo in patients undergoing radiotherapy for breast cancer. Phys Imaging Radiat Oncol 2018;5:97–101.

[10] Dzierma Y, Mikulla K, Richter P, Bell K, Melchior P, Nuesken F, et al. Imaging dose and secondary cancer risk in image-guided radiotherapy of pediatric patients. Radiat Oncol 2018;13(1). https://doi.org/10.1186/s13014-018-1109-8.

[11] Xu XG, Bednarz B, Paganetti H. A review of dosimetry studies on external-beam radiation treatment with respect to second cancer induction. Phys Med Biol 2008; 53(13):R193–241.

[12] Kry SF, Bednarz B, Howell RM, Dauer L, Followill D, Klein E, et al. AAPM TG 158: Measurement and calculation of doses outside the treated volume from external-beam radiation therapy. Med Phys. 2017;44:e391-e429.

[13] Taylor MichaelL, Kron T. Consideration of the radiation dose delivered away from the treatment field to patients in radiotherapy. J Med Phys 2011;36(2):59. https://doi.org/10.4103/0971-6203.79686.

[14] De Saint-Hubert M, Verellen D, Poels K, Crijns W, Magliona F, Depuydt T, et al. Out-of-field doses from pediatric craniospinal irradiations using 3D-CRT, IMRT, helical tomotherapy and electron-based therapy. Phys Med Biol 2017;62(13): 5293–311.

[15] Taylor ML, Kron T, Franich RD. Assessment of out-of-field doses in radiotherapy of brain lesions in children. Int J Radiat Oncol Biol Phys 2011;79(3):927–33.

[16] De Saint-Hubert M, Majer M, Hraak H, Heinrich Z, Knecevic Z, Miljanic S, et al. Out-of-field doses in children treated for large arteriovenous malformations using hypofractionated gamma knife radiosurgery and intensity-modulated radiation therapy. Radiat Prot Dosimetry. 2018;181:1-11.

[17] Xiao Y, Kry SF, Popple R, Yorke E, Papanikolaou N, Stathakis S, et al. Flattening filter-free accelerators: a report from the AAPM Therapy Emerging Technology Assessment Work Group. J Appl Clin Med Phys 2015;16(3):12–29.

[18] Kragl G, Baier F, Lutz S, Albrich D, Dalaryd M, Kroupa B, et al. Flattening filter free beams in SBRT and IMRT: dosimetric assessment of peripheral doses. Z Med Phys 2011;21(2):91–101.

[19] Duggan L, Hood C, Warren-Forward H, Haque M, Kron T. Variations in dose response with x-ray energy of LiF:Mg, Cu, P thermoluminescence dosimeters: implications for clinical dosimetry. Phys Med Biol 2004;49(17):3831–45.

[20] Lonski P, Keehan S, Siva S, Pham D, Franich RD, Taylor ML, et al. Out-of-field in vivo dosimetry using TLD in SABR for primary kidney cancer involving mixed photon fields. Phys Med 2017;37:9–15.

[21] Lonski P, Taylor ML, Franich RD, Harty P, Kron T. Assessment of leakage doses around the treatment heads of different linear accelerators. Radiat Prot Dosimetry 2012;152(4):304–12.

[22] Mazonakis M, Zacharopoulou F, Varveris H, Damilakis J. Peripheral dose measurements for 6 and 18 MV photon beams on a linear accelerator with multileaf collimator. Med Phys 2008;35(10):4396–403.

[23] Vassiliev ON, Titt U, Pönisch F, Kry SF, Mohan R, Gillin MT. Dosimetric properties of photon beams from a flattening filter free clinical accelerator. Phys Med Biol 2006;51(7):1907–17.

[24] Klein EE, Maserang B, Wood R, Mansur D. Peripheral doses from pediatric IMRT. Med Phys 2006;33(7Part1):2525–31.

[25] Lonski P, Taylor ML, Franich RD, Kron T. A collimated detection system for assessing leakage dose from medical linear accelerators at the patient plane. Australas Phys Eng Sci Med 2014;37(1):15–23.

[26] Wijesooriya K. Part I: out-of-field dose mapping for 6X and 6X-flattening-filter-free beams on the TrueBeam for extended distances. Med Phys 2019;46(2):868–76.

[27] Covington EL, Ritter TA, Moran JM, Owrangi AM, Prisciandaro JI. Technical report: evaluation of peripheral dose for flattening filter free photon beams. Med Phys 2016;43(8Part1):4789–96.

[28] Kry SF, Vassiliev ON, Mohan R. Out-of-field photon dose following removal of the flattening filter from a medical accelerator. Phys Med Biol 2010;55(8):2155–66.

[29] Hall EJ. Intensity-modulated radiation therapy, protons, and the risk of second cancers. Int J Radiat Oncol Biol Phys 2006;65(1):1–7.

[30] Darby SC, Ewertz M, McGale P, Bennet AM, Blom-Goldman U, Brønnum D, et al. Risk of ischemic heart disease in women after radiotherapy for breast cancer. N Engl J Med 2013;368(11):987–98.